JOURNAL OF GEOPHYSICAL RESEARCH, VOL. 115, B01403, doi:10.1029/2009JB006546, 2010

Click Here for Full Article

Global mass flux solutions from GRACE: A comparison of parameter estimation strategies—Mass concentrations versus Stokes coefficients

D. D. Rowlands,[1] S. B. Luthcke,[1] J. J. McCarthy,[2] S. M. Klosko,[2] D. S. Chinn,[2] F. G. Lemoine,[1] J.-P. Boy,[1,3] and T. J. Sabaka[1]

Received 16 April 2009; revised 27 August 2009; accepted 25 September 2009; published 27 January 2010.

[1] The differences between mass concentration (mascon) parameters and standard Stokes coefficient parameters in the recovery of gravity information from gravity recovery and climate experiment (GRACE) intersatellite K-band range rate data are investigated. First, mascons are decomposed into their Stokes coefficient representations to gauge the range of solutions available using each of the two types of parameters. Next, a direct comparison is made between two time series of unconstrained gravity solutions, one based on a set of global equal area mascon parameters (equivalent to $4° \times 4°$ at the equator), and the other based on standard Stokes coefficients with each time series using the same fundamental processing of the GRACE tracking data. It is shown that in unconstrained solutions, the type of gravity parameter being estimated does not qualitatively affect the estimated gravity field. It is also shown that many of the differences in mass flux derivations from GRACE gravity solutions arise from the type of smoothing being used and that the type of smoothing that can be embedded in mascon solutions has distinct advantages over postsolution smoothing. Finally, a 1 year time series based on global 2° equal area mascons estimated every 10 days is presented.

Citation: Rowlands, D. D., S. B. Luthcke, J. J. McCarthy, S. M. Klosko, D. S. Chinn, F. G. Lemoine, J.-P. Boy, and T. J. Sabaka (2010), Global mass flux solutions from GRACE: A comparison of parameter estimation strategies—Mass concentrations versus Stokes coefficients, *J. Geophys. Res.*, *115*, B01403, doi:10.1029/2009JB006546.

1. Introduction

[2] Over the years mass concentration (mascon) parameters have been used by researchers to model variations in planetary gravity fields. *Muller and Sjogren* [1968] were probably the first to identify planetary surface mascons from tracking data, and then *Wong et al.* [1971] estimated mascon parameters directly from satellite tracking data. They found that mascons were ideal parameters for lunar gravity recovery in conditions of uneven geographical tracking coverage. *Rapp* [1974] formally addressed the use of satellite observations to estimate regional gravity models in the form of gravity anomalies, with *Rummel et al.* [1978] extending this concept to satellite-to-satellite tracking configurations. More recently, *Rowlands et al.* [2005] and *Luthcke et al.* [2006a, 2008] applied a mascon technique optimized for the unique characteristics of the gravity recovery and climate experiment (GRACE) mission [*Tapley et al.*, 2004] to estimate time variable gravity solely from GRACE intersatellite tracking data. They found that mascons significantly improved the spatial and temporal resolution achievable from the GRACE intersatellite K-band range rate (KBRR) observations when using correlation constraint equations in least squares solutions. These recent mascon studies were used to recover regional mass flux and are computationally convenient because they can be estimated from a small subset of the global GRACE KBRR data.

[3] To study mass balance from GRACE in a region such as Greenland, many researchers have used the standard GRACE mission Level 2 monthly Stokes coefficients as the fundamental data type. Some of the first Level 2 Stokes coefficient based derivations of mass flux over Greenland, for example by *Velicogna and Wahr* [2006], used Gaussian smoothing and averaging kernels estimating only trends in mass flux over only the northern and southern subregions of Greenland. More recently, *Wouters et al.* [2008] used Gaussian smoothing and a forward model "fingerprinting" technique to gain increased spatial and temporal resolution from the GRACE Level 2 Stokes coefficients. Using this approach, they were able to derive mass flux estimates (including trend and average annual signal) in individual drainage basins similar to the drainage basins used in the mascon-based approach of *Luthcke et al.* [2006a] (an approach in which mass flux is estimated directly from GRACE Level 1B tracking data). Although the two approaches (Stokes coefficients with fingerprinting and mascons) have yielded similar results for mass trends in the drainage basins (and Greenland overall), the mascon

[1]Planetary Geodynamics Laboratory, NASA Goddard Space Flight Center, Greenbelt, Maryland, USA.
[2]SGT Inc., Greenbelt, Maryland, USA.
[3]EOST-IPGS, UMR 7516, Université de Strasbourg, CNRS, Strasbourg, France.

Copyright 2010 by the American Geophysical Union.
0148-0227/10/2009JB006546$09.00

approach has revealed more information about interannual variability in the subregions than any Stokes coefficient based approach. *Luthcke et al.* [2006a] produced time series of mass flux in each drainage basin with a temporal resolution of 10 days revealing each year's distinct melt and accumulation seasons. Furthermore, the mascon-based approach of *Luthcke et al.* [2008] was able to produce a time series of mass flux over individual Alaska glaciers at 2° spatial and 10 day temporal resolution. To date no spherical harmonic based approach for mass flux derivation from GRACE has been demonstrated to produce that type of resolution. One of the goals of this paper is to investigate the nature of the differences in recovered mass flux from Stokes coefficients and from mascons.

[4] One of the problems with comparing Stokes coefficients and mascons that have been estimated from GRACE data is that most GRACE mascon solutions have been regional, estimating only a few parameters from a small subset of the GRACE data (limited to the coverage of the region of interest). In this paper, we estimate two global sets of mascons (one with 4° spatial resolution and the other at 2° spatial resolution). As will be shown in subsequent sections, these mascon solutions easily translate into Stokes coefficients that can be compared to Stokes coefficients that have been estimated as individual parameters. This paper will have the following format. First, we will describe the mascon formulation and its relationship to the underlying spherical harmonic basis functions. Second, we compare Stokes coefficients from a standard solution to Stokes coefficients that have been reconstituted from a 4° global mascon solution (with each solution using the same data and fundamental data processing prior to estimation). Finally, we provide results for a 2° equal area global mascon solution using its corresponding spherical harmonic representation. This 2° global mascon solution uses specialized sets of regional smoothing constraint equations in the least squares solution along with the standard observation equations. This reconstituted spherical harmonic solution does not require postsolution mitigation techniques, such as Gaussian smoothing and averaging kernels, in order to be used in mass flux computations.

2. Mascon Formulations

[5] Mascon parameters are used to obtain a geographically specific correction to a global mean gravity field. Each mascon parameter represents a surplus or deficit of surface mass (as compared to the a priori mean field and forward models) in a predetermined region over a specified time interval. Each mascon region is usually (but not necessarily) a regularly shaped area like a rectangular cell. The surplus or deficit of mass in the region is represented as a uniform mass layer (expressed in centimeters of equivalent water) over that region. In other words, mascons represent surface mass distribution as spatial and temporal step functions.

[6] In order to recover a gravity parameter from satellite tracking data, it is necessary to relate the orbital motion of each satellite participating in an observation to gravity parameters. The procedure for relating standard Stokes coefficients to orbital motion is universal and is the backbone of almost all satellite tracking data analysis. We start with the potential at satellite altitude computed from the Stokes coefficients:

$$U(r,\vartheta,\lambda) \approx \frac{GM}{R}\left[\sum_{t=1}^{l_{\max}}\sum_{m=0}^{l}\left(\frac{R}{r}\right)^{l+1}\overline{P}_{lm}(\sin\vartheta)\right. \left(\overline{C}_{lm}\cos m\lambda + \overline{S}_{lm}\sin m\lambda\right), \tag{1}$$

where r, ϑ, and λ are the spherical geocentric radius, latitude, and longitude coordinates of the point where the geopotential is evaluated; GM is the product of the universal gravitational constant, G and the Earth's mass, M; R is the Earth's mean semi-major axis; l and m are the spherical harmonic degree and order; $\overline{P}_{lm}$ are the fully normalized associated Legendre functions; and $\overline{C}_{lm}$, $\overline{S}_{lm}$ are the fully normalized Stokes coefficients.

[7] Mascon parameters are less commonly used, and the method for relating them to orbital motions varies among researchers. What is common among users of mascons is the need to upward continue the gravitational potential associated with the differential mass distribution at the Earth's surface to satellite altitude. This differential mass distribution is composed of a direct effect arising from the addition of a layer of surface mass and an indirect effect arising from the redistribution of the original underlying surface mass (caused by the loading of the additional surface mass). The formulation for mascon parameters is derived from the fact that a change in the gravitational potential caused by adding a small uniform layer of mass over a region, j, at an epoch t can be represented as a set of (differential) potential coefficients which can be added to the mean field. The delta coefficients can be computed (*Chao et al.*, 1987):

$$\begin{aligned}\Delta\overline{C}_{jlm}(t) &= \frac{\sigma_j(t)\left(1+k'_l\right)R^2}{(2l+1)M}\int \overline{P}_{lm}(\sin\vartheta)\cos\ m\lambda\, d\Omega \\ \Delta\overline{S}_{jlm}(t) &= \frac{\sigma_j(t)\left(1+k'_l\right)R^2}{(2l+1)M}\int \overline{P}_{lm}(\sin\vartheta)\sin\ m\lambda\, d\Omega\end{aligned}, \tag{2}$$

where the evaluation of the integrals is restricted to region j; k'_l is the loading Love number of degree l, to account for the Earth's elastic yielding which in general counteracts the additional surface density; $\sigma_j(t)$ is the mass of the layer over a unit of surface area at the epoch, t, for region, j; Ω is the solid angle surface area of the region where $\sigma_j(t)$ is applied, $d\Omega = \cos\vartheta\ d\vartheta\ \vartheta\lambda$.

[8] In principle, there can be various ways to upward continue this gravitational potential, but equation (2) conveniently relates the additional surface mass (including loading) to standard Stokes coefficients, making upward continuation convenient and straightforward for tracking data analysis.

[9] The units of $\sigma_j(t)$ are kg/m^2, and this quantity can be rewritten as $10 \times H_j(t)$ where $H_j(t)$ represents the height of a uniform layer of water over region, j, expressed in centimeters. The factor of 10 arises from the fact that a layer of water 1 cm deep over 1 m^2 has a mass of 10 kg. $H_j(t)$ is our mascon parameter for the jth mascon region. The epoch, t, associated with the mascon parameter is a representative

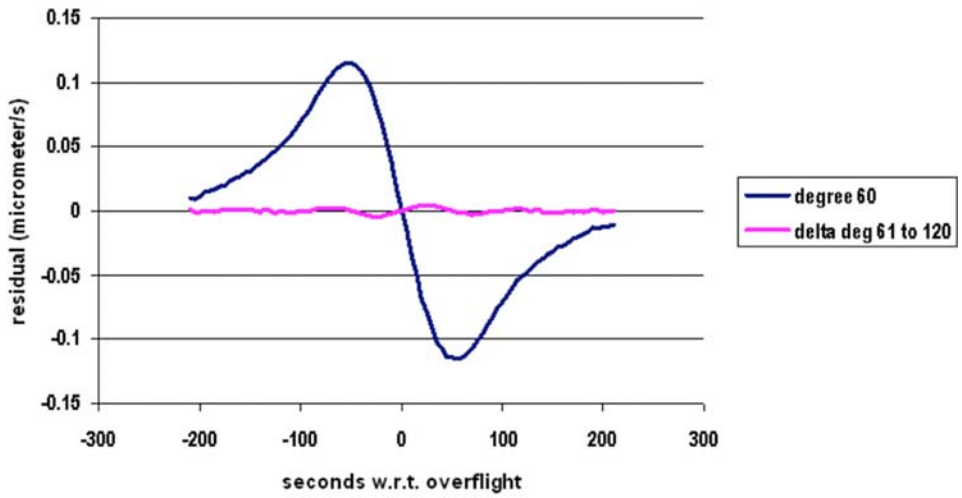

Figure 1. Simulated GRACE KBRR observations for a direct overflight of a 4° × 4° block having a surplus water height of 20 cm. Shown are the observations for a field truncated to degree 60 and the difference in the observations if the field is extended to degree 120.

time tag (usually the center point) over an interval (usually 10 days) where we treat the layer as invariant. Equation (2) can be rewritten in terms of our mascon parameter, $H_j(t)$:

$$\Delta C_{jlm}(t) = H_j(t)*\left[\frac{10*(1+k_l')R^2}{(2l+1)M}\right]\int \overline{P}_{lm}(\sin\ \vartheta)\cos\ m\lambda\ \delta\Omega$$
$$\Delta S_{jlm}(t) = H_j(t)*\left[\frac{10*(1+k_l')R^2}{(2l+1)M}\right]\int \overline{P}_{lm}(\sin\vartheta)\sin\ m\lambda\ \delta\Omega. \tag{3}$$

$H_j(t)$ is the mascon parameter of the jth region at time, t, and it is a scalar. It is also possible to create a global height function associated with the jth mascon region at time, t, from the delta Stokes coefficients computed in equation (3). Equation (4) has been modified slightly from *Wahr et al.* [1998] to express mass per unit area in terms of a layer of water in centimeters:

$$H_j(\vartheta\lambda t) = \left[\frac{M}{40\pi R^2}\right]*\sum_{l=0}^{\infty}\left(\frac{2l+1}{1+k_l}\right)\sum_{m=0}^{1} \cdot \overline{P}_{lm}(\sin\vartheta)*\left[\Delta C_{jlm}\cos\ m\lambda + \Delta S_{jlm}\sin\ m\lambda\right]. \tag{4}$$

If equation (4) is evaluated to a sufficient degree and order, then, $H_j(\theta,\ \lambda,\ t)$ becomes a step function with:

$$H_j(\vartheta,\lambda,t) = H_j(t) \text{ if } (\vartheta.\lambda) \text{ is in region } j$$

sand

$$H_j(\vartheta,\lambda,t) = 0 \text{ if } (\vartheta.\lambda) \text{ is not in region } j.$$

From equation (3), it is clear that there is a strictly linear relationship between the height of a uniform layer of water over a region (in other words, a mascon parameter) and the resulting change it induces in each and every Stokes coefficient. Also from equation (4), it should be clear that each mascon parameter can be represented as a scale factor applied to a set of precomputed (as given by equation (3) with $H_j(t)$ set to unity) "delta" Stokes coefficients. Of course, there are various ways to relate orbital motions to mascons, but equation (4) shows that any mascon parameter, regardless of the method used for upward continuation, is equivalent to a scale factor on a set of precomputed Stokes coefficients. Also, each partial derivative of the KBRR tracking observation with respect to a mascon parameter is a linear combination of the partials of the tracking measurements with respect to standard Stokes coefficients. The multipliers in the linear combination are the Stokes coefficients in the base set of differential coefficients [*Rowlands et al.*, 2005].

[10] From equations (3) and (4), it should also be clear that there can be only two differences between any pair of representations of gravity through mascons: the regions chosen (size, shape, and location) for the mascons and the degree to which mass is represented as a step function (for the Stokes coefficient representation of mascons, this corresponds to the maximum degree used in the set of "delta" coefficients). Although the maximum degree used for sets of precomputed Stokes coefficients is a factor in differentiating between mascon representations, for the purpose of most GRACE modeling, there is not much difference above degree 60. For example, the Stokes coefficients above degree 60 in a 4° × 4° mascon block do not contribute significantly to modeled GRACE intersatellite range rate measurements nor to the estimation of mascon parameters from GRACE intersatellite range-rate measurements (see Figure 1). All mascons described in this study are based on Stokes coefficients computed to degree 60.

[11] A mascon-based technique for gravity recovery from tracking data depends not only on the representation used for surface mascons, but also on the least squares estimation scheme used to estimate the parameters and in some cases, on postsolution smoothing. Mascon parameters are particularly easy to use with various types of constraint equations. Therefore, despite commonality among mascon representations, there is a wide variety of mascon-based techniques for gravity estimation differing mainly in the use of smoothing techniques. Gaussian smoothing applied after the gravity

solution is probably the most common type of smoothing in use, but in this study we also explore smoothing through the use of constraint equations embedded in the gravity solution. In this study, we will compare solutions for global mascons which have been estimated with and without the use of embedded constraint equations, to solutions for standard Stokes coefficients through degree 60. All the solutions in the study use the same fundamental processing of GRACE intersatellite KBRR data as described in *Luthcke et al.* [2006b].

[12] The fundamental processing occurs in two steps with the calibration of the GRACE accelerometers taking place in preliminary solutions. In these preliminary solutions, GRACE KBRR data and GRACE precise ephemeris data (the GNV1B data product) are reduced simultaneously in daily arcs to estimate the full initial state (12 parameters) of the two GRACE satellites along with 28 accelerometer biases for each of the two GRACE satellites. For each satellite, a X (along track) bias, a Z (radial) bias, and a 1-cycle per revolution X bias are estimated every 3 h while a Y (cross track) bias and a scale bias for each axis are estimated every 24 h. The second run reduces only GRACE KBRR data and estimates only 3 of the 12 GRACE initial state vector elements expressed as baseline parameters as in *Rowlands et al.* [2002] while holding the accelerometer biases fixed to the values determined in the first run. When the solution for the initial state is converged, a file is written that contains observation residuals and partial derivatives of the computed KBRR observations with respect to parameters of the initial state and of Stokes coefficients through degree 60. This file is used in later steps to generate normal equations for Stokes coefficients and also for mascons. This ensures that the fundamental processing is the same for both types of gravity parameters. In all of the fundamental processing, mean gravity is modeled with the GGM02C gravity field [*Tapley et al.*, 2005]. Gravity variations from the atmosphere are modeled to degree and order 90 at 3 hour intervals derived from European Centre for Medium-Range Weather Forecasts (ECMWF) operational pressure grids. Ocean tides are modeled with the GOT4.7 tide model [*Ray*, 1999; *Ray and Ponte*, 2003]. The nonbarotrophic response of the ocean to atmospheric pressure loading (derived from 6 hourly ECMWF atmospheric pressure and winds), is modeled to degree and order 90 using MOG2D [*Carrere and Lyard*, 2003]. Finally, it should be mentioned that all of the gravity solutions presented in this paper co-estimate the same set of nongravitational parameters. These are three GRACE initial state baseline parameters for each day.

3. Mascons Versus Stokes Coefficients

[13] Given the fact that mascons are essentially scale factors on sets of precomputed Stokes "delta" coefficients, it is natural to wonder if there is any difference between the estimation of mascon parameters and the estimation of individual Stokes coefficients in the recovery of gravity from satellite tracking data. One obvious difference is that mascon parameters can be used to estimate regional solutions, while individual Stokes coefficients are global in nature. However, when mascons are estimated over the entire Earth (as global mascons), a set of global Stokes coefficients is also being estimated, not as individual parameters, but as linear combinations of sets of precomputed "delta" Stokes coefficients. This is evidence that unconstrained global mascon solutions are not so different from unconstrained solutions for a global representation of the gravity field using Stokes coefficients. It also makes the comparison of global mascon solutions to solutions based on standard Stokes coefficients very convenient.

[14] The first set of mascon solutions in this study use a global grid of equal area cells on which each cell has an area nearly equal to a 4° rectangle at the equator. The grid is composed of rectangles in 4° latitude bands everywhere except for a 2° spherical cap at each pole. Each solution based on this grid estimates 2586 mascons, each of which uses Stokes coefficients computed through degree 60. Each of these 2586 mascon parameters is a scale factor on a function describing the thickness of surface mass (having the density of water) over the sphere. These 2586 surface mass functions form a linearly independent set of functions. Each of these functions is in turn a linear combination of the 3720 spherical harmonic functions through degree 60. Of course, each individual spherical harmonic function also describes surface mass, and the collection of these through degree 60 also forms a linearly independent set of functions. It is clear that the functional space spanned by the 3720 spherical harmonic functions maps onto (a subset of it describes perfectly) the functional space spanned by the 2586 surface mass functions associated with the global mascon parameters. It is also clear that the space spanned by the 2586 mascon functions maps into (but not entirely onto) the functional space spanned by the 3720 spherical harmonic functions. In other words, the set of solutions available through mascon parameters based on the grid described above is a proper subset of the solutions available through the estimation of individual Stokes coefficients through degree 60.

[15] The above comparison could be altered so that the mascon parameters occupy the same grid points but are represented using Stokes coefficients only through degree 50. One would expect that any unconstrained solution based on these parameters would closely resemble a solution for individually estimated Stokes coefficients through degree 50. In this case the number of linearly independent functions on which each solution is based is nearly the same (2586 versus 2600). As above, it is not only that the dimensions of the functional vector spaces are close, but also every function described by a mascon solution is exactly equivalent to a linear combination of spherical harmonics. Even though this "50–50" comparison has the best chance for equivalence, our study compares mascons computed with coefficients through degree 60 to monthly solutions for standard Stokes coefficients estimated through degree 60. These are the most common types of gravity solutions found in the GRACE literature.

4. A Direct Comparison of Gravity Solutions: 4° Equal Area Global Mascons Versus Stokes Coefficients

[16] In this section, we compare time series of monthly global gravity solutions estimated from GRACE intersatellite tracking data. Each time series is composed of 13 months from July 2003 through July 2004, and all of the individual

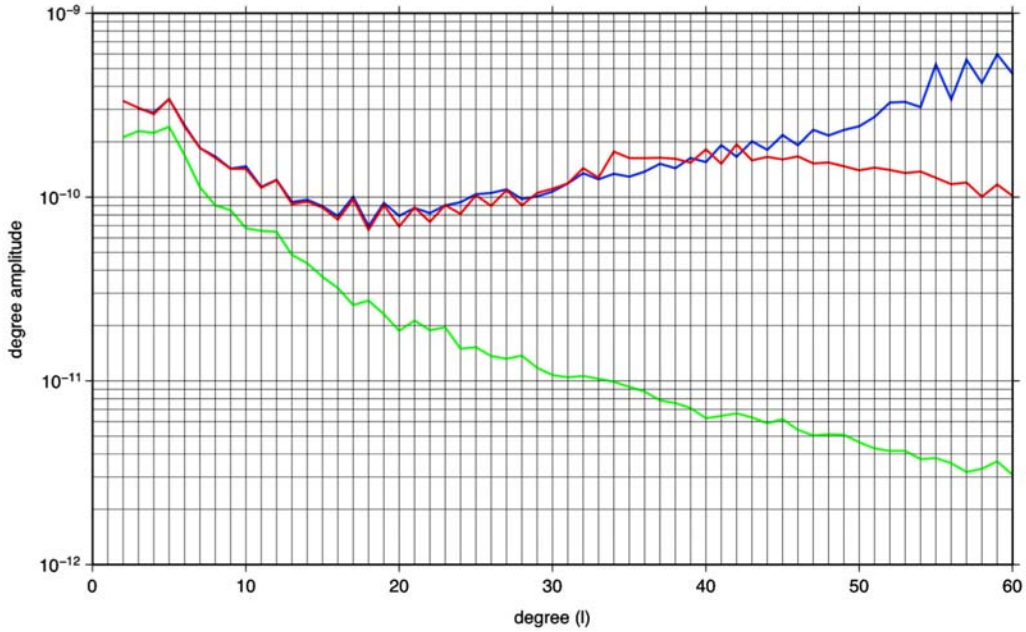

Figure 2. Power spectra of changes with respect to the GGM02C gravity field and forward models of the unconstrained standard spherical harmonic solution and the unconstrained 4° mascon solution (both from the same GRACE KBRR data) compared to the GLDAS surface hydrology model. The blue curve represents the coefficients of the standard solution, the red curve represents the delta Stokes coefficients of the global mascons, and the green represents the coefficients of the GLDAS surface hydrology model. Given that atmospheric pressure and tidal mass flux signals are forward modeled in these solutions, the expected spectra of the gravity fields should be similar to the spectrum of global hydrology.

monthly solutions use the same GRACE observation processing scheme which is described in *Luthcke et al.* [2006b]. The key point about the comparisons described in this section is that the normal equations for any monthly solution in one series were formed using exactly the same observation residuals as the normal equations for the same month in any other series. Our first comparison will be between two time series of unconstrained and unsmoothed solutions, one estimating mascons and the other directly estimating individual Stokes coefficients, each series using the same GRACE KBRR data. Because the fundamental processing is the same in each series, any differences, especially in the lower degrees and orders of the estimated gravity fields can be attributed directly to the type of parameters being estimated and to a lesser extent the exact number of parameters being estimated in each solution (2856 mascons versus 3720 Stokes coefficients). After this first comparison, we will compare the time series when various smoothing techniques, including constraint equations, have been applied.

[17] We will look at several aspects of each time series of monthly global gravity solutions: (1) Stokes coefficient values (whether directly estimated or reconstructed from mascon parameters) at degree 2 and at degree and order 15, (2) the degree variances of the Stokes coefficients, and (3) the geographical distribution of the standard deviation of the derived mass signal. Coefficients are compared at degree 2 as a measure of the agreement among time series at long wavelength. The resonance terms at degree and order 15 for the GRACE satellites are well known as a source of aliasing problems in GRACE gravity time series [cf. *Swenson and Wahr*, 2006; *Luthcke et al.*, 2006b], so a comparison of these coefficients is especially relevant. Because hydrology is a major component of global mass flux sensed by GRACE [*Chen et al.*, 2006], the degree variances of each gravity time series will be compared to the degree variances of the time series of Stokes coefficients of the GLDAS hydrology model [*Rodell et al.*, 2004]. One would expect that the signal from global time variable gravity has more power at every degree than the signal from hydrology alone, but the power spectrum from a time series of gravity solutions should not deviate greatly from that of hydrology (tides and atmospheric pressure variations were forward modeled). As will be seen below, constraint equations and smoothing techniques can be used to "tune" the power spectrum of a gravity time series as well as to smooth the geographical distribution of the standard deviation of the derived mass signal. However, it is not necessarily true that the optimization of one criterion will benefit the other. For each time series, we will examine the compatibility of the power spectrum with the spatial distribution of the standard deviation of the mass signal.

[18] Figure 2 gives strong evidence that the two unconstrained global solutions (mascons and Stokes coefficients) are very similar. The power spectra of the two solutions are almost identical through degree 30 and very similar through degree 40. Figures 3a through 3e show that individual coefficients at degree 2 and at degree and order 15 are nearly identical. In other words, the solutions are the same at long wavelength and have the same problem at this resonance degree and order. To demonstrate the severity of the problem at this resonance degree and order, the time

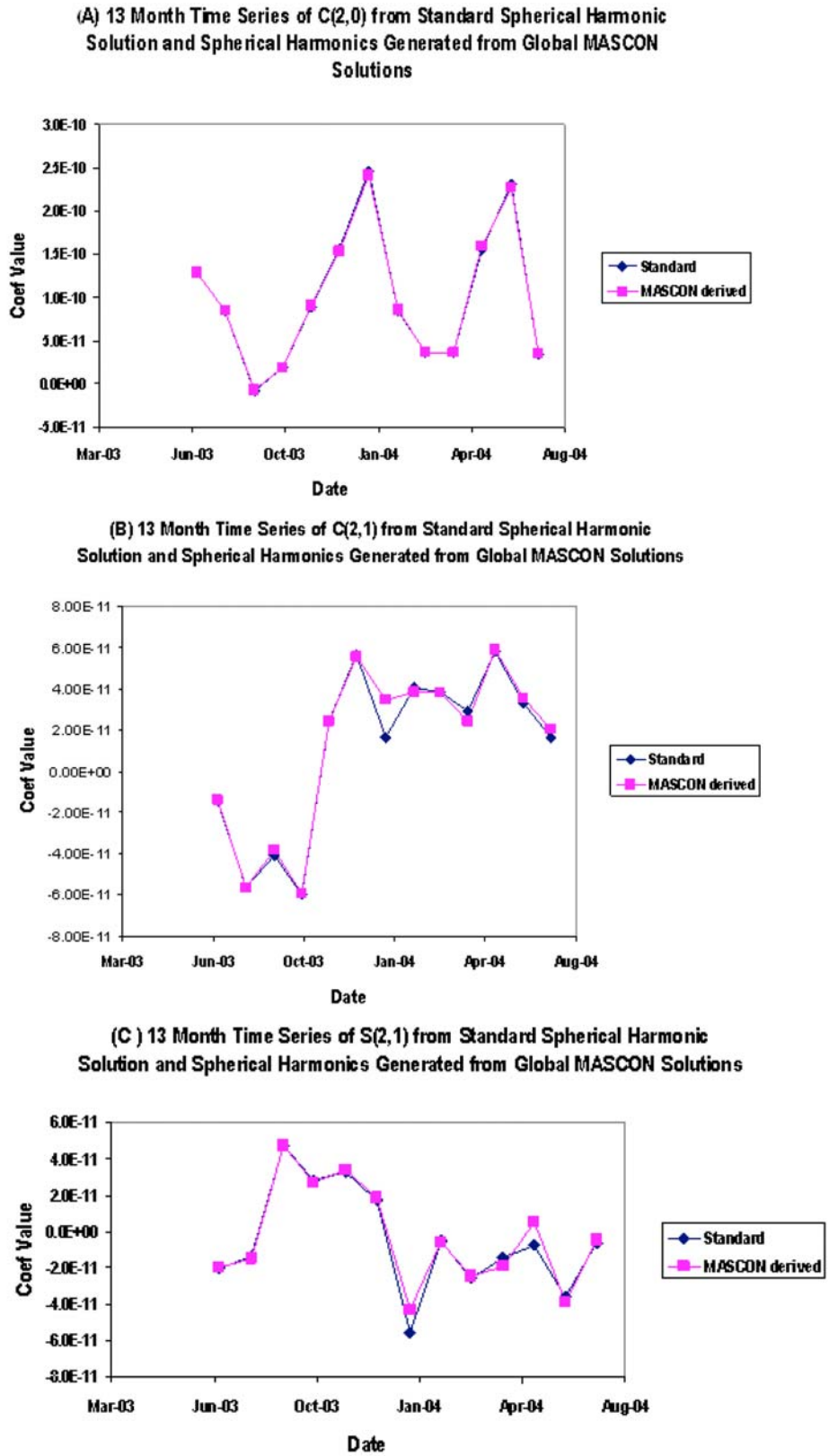

Figure 3. Spherical harmonic coefficients estimated individually in a standard unconstrained solution and the spherical harmonics given by an unconstrained global 4° mascon solution. The longest wavelength terms, (a) $C(2, 0)$, (b) $C(2, 1)$ and (c) $S(2, 1)$. (d) $C(15,15)$ and (e) $S(15,15)$ coefficients, which are the dominant resonance terms. These are obtained from unconstrained solutions. In Figures 3d and 3e, the GLDAS coefficients have been plotted in green to demonstrate the nongeophysical behavior of the resonance terms from month to month.

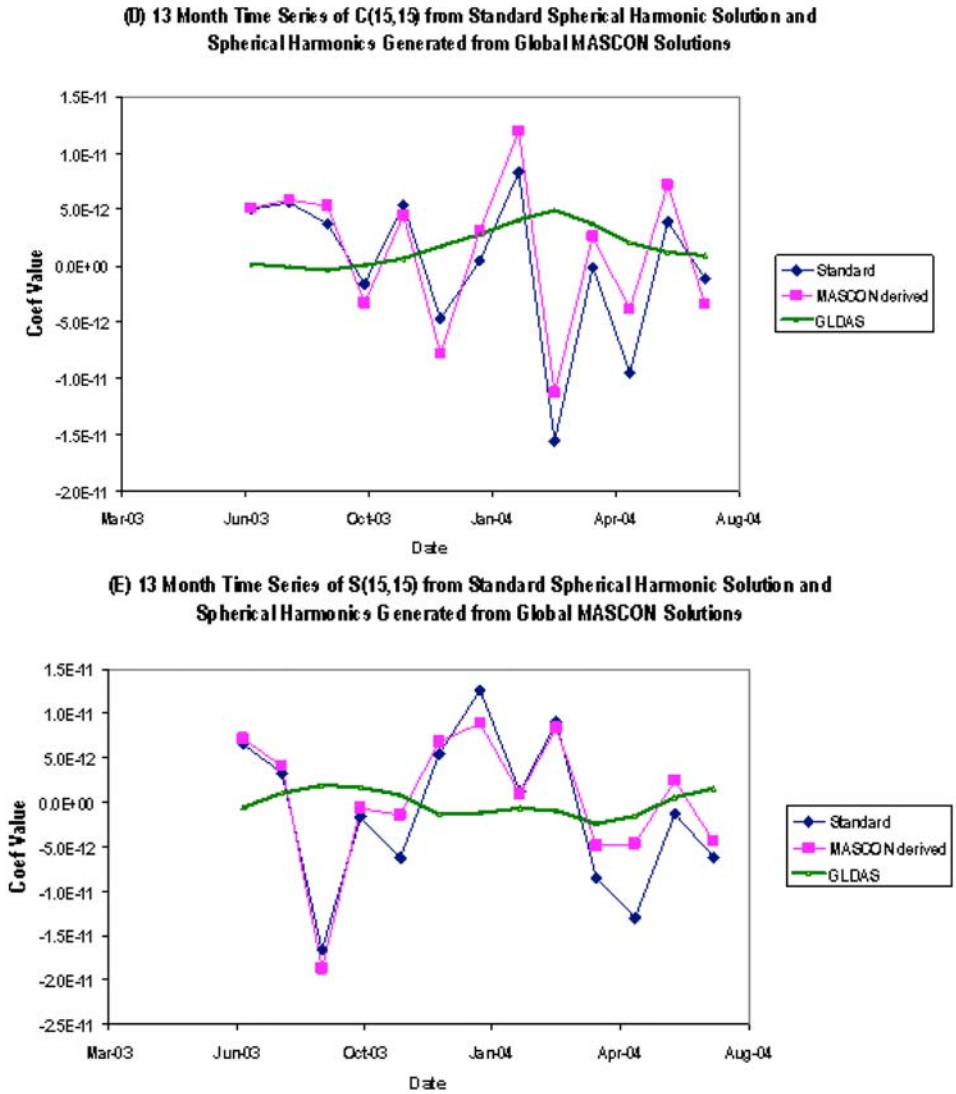

Figure 3. (continued)

series of the GLDAS hydrology coefficients are also plotted in Figures 3d and 3e. Both solutions need some type of smoothing before the geographical distribution of the standard deviation of the derived mass signal shows reasonable patterns. The smallest Gaussian smoothing radius which produces a reasonable pattern for either solution is roughly 500 km. Figures 4 and 5 show the geographical distribution of the standard deviation of the derived mass signal for each solution using Gaussian smoothing at 500 km. There is not much difference. Although the distribution of mass signal for these solutions looks reasonable, Figure 6 shows that the power spectra of both smoothed solutions are reasonable in comparison to GLDAS hydrology until only about degree 30, after which the signal begins to fall off rapidly.

[19] In order to keep the GRACE solutions' power spectra above hydrology at all degrees through 60, it is necessary to decrease the Gaussian smoothing radius to about 400 km (even at 400 km the mascon power spectrum dips below hydrology at the upper degrees). When the solutions are Gaussian smoothed with a radius of 400 km, the power spectra shown in Figure 7 more closely resemble the GLDAS power spectrum, although the solution spectra are fairly high relative to GLDAS at mid-degrees. We could further seek the optimal smoothing radius to dampen the power at mid-degrees, but then the power would be significantly reduced at the higher degrees as seen in our previous example using a smoothing radius equal to 500 km. Furthermore, Figures 8 and 9 show that smoothing with a radius of 400 km does not take care of the dominant resonance errors. Figures 8 and 9 reveal streaks in the oceans and in the desert areas like the Arabian Peninsula and interior Australia. Comparing Figures 3d and 3e with Figure 10 shows that Gaussian smoothing does not significantly reduce the nongeophysical nature of the time series of the degree 15 and order 15 resonance. The smoothed time series of this resonance is very similar to the unsmoothed time series. The smoothed time series of this resonance are dampened a bit, but continue to show too much variation from month to month. There is an incompatibility between power and mass distribution that Gaussian smoothing cannot resolve because it cannot reduce the variance at the resonance degrees and orders while preserving the

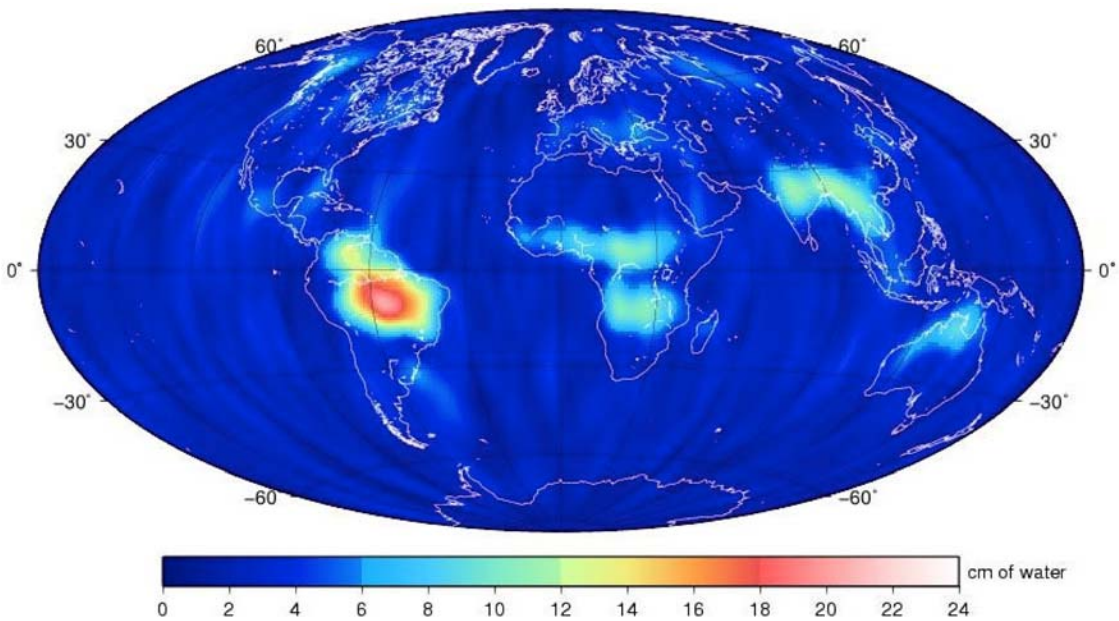

Figure 4. The standard deviation of surface mass (expressed as standing water height) obtained from 13 monthly solutions directly estimating a 60 × 60 standard gravity field from the GRACE KBRR data. Atmospheric pressure and tidal mass flux have been forward modeled. These monthly solutions are unconstrained, but have been Gaussian smoothed with a radius of 500 km.

power at the higher degrees. Previous studies have sought to mitigate this problem using filtering methods applied to each spectral coefficient time series after the gravity estimation process and without connection to the GRACE KBRR data [*Swenson and Wahr*, 2006]. We will show that mascon constraint equations provide a method to effectively solve this problem within the time variable gravity estimation process while minimizing the GRACE KBRR residuals.

[20] We now examine the above global mascon solution with the addition of spatial constraint equations. Some mascon solutions such as described by *Rowlands et al.*

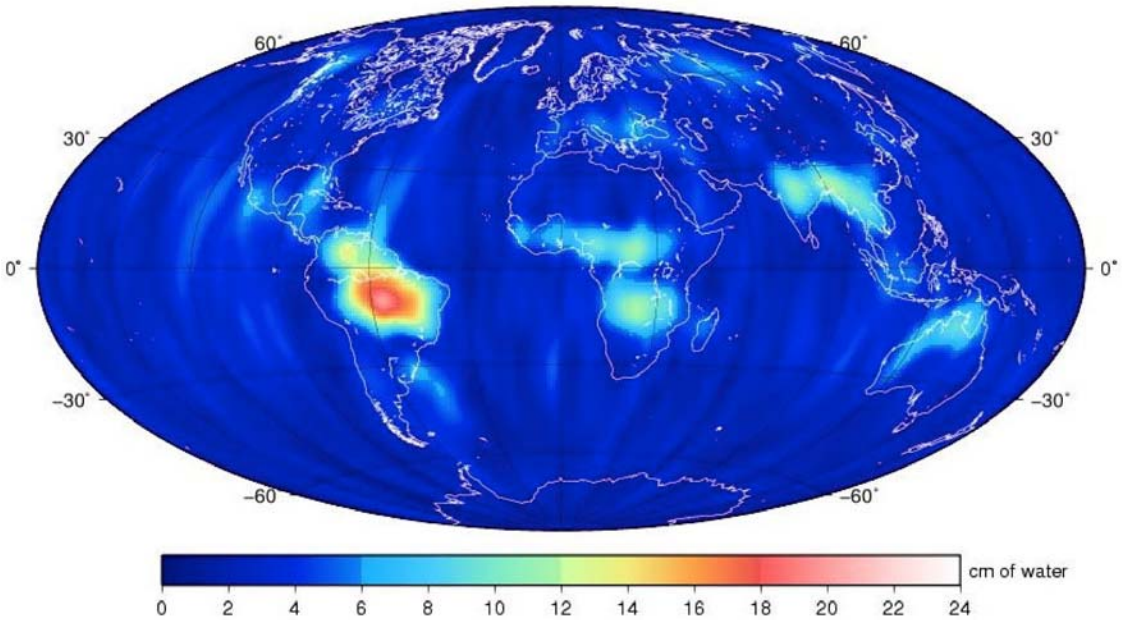

Figure 5. The standard deviation of surface mass (expressed in standing water height) obtained from 13 monthly solutions estimating 4° mascons from GRACE KBRR data. The delta coefficients have been reconstituted through degree and order 60. Atmospheric pressure and tidal mass flux have been forward modeled. These monthly solutions are unconstrained, but have been Gaussian smoothed with a radius of 500 km.

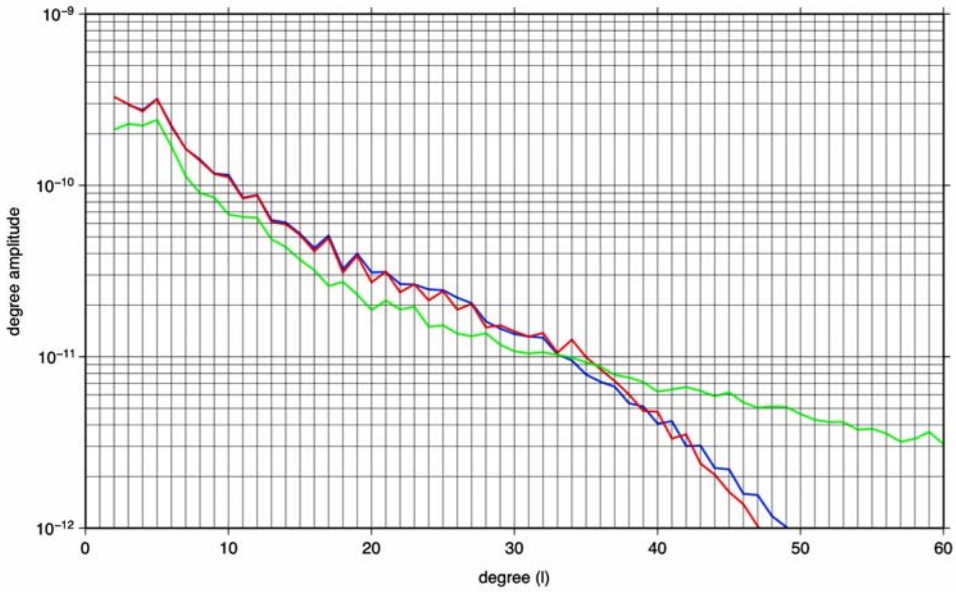

Figure 6. Power spectra of changes with respect to the GGM02C gravity field and forward models of the unconstrained standard spherical harmonic solution and the unconstrained 4° MASCON solution (both from the same GRACE KBRR data) compared to the GLDAS surface hydrology model. Both solutions have been postprocessed through Gaussian smoothing using a cap radius of 500 km. The blue curve represents the coefficients of the standard solution, the red curve represents the delta Stokes coefficients of the global mascons, and the green curve represents the coefficients of the GLDAS surface hydrology model (no smoothing). Given that atmospheric pressure and tidal mass flux signals are forward modeled in these solutions, the expected spectra of the gravity fields would be similar to the spectrum of the global hydrology. Gaussian smoothing has reduced the power of the high degree terms to unrealistic levels above degree 35.

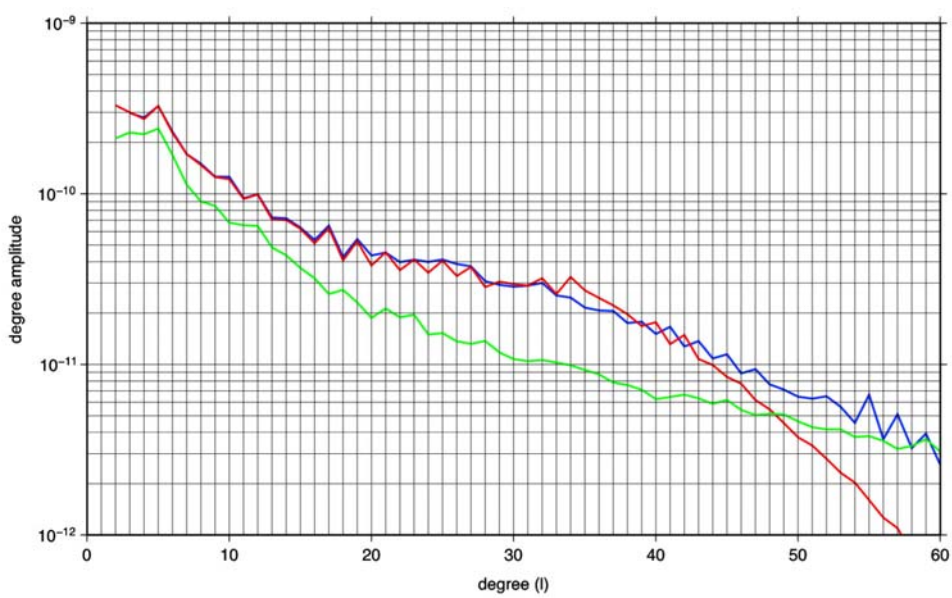

Figure 7. Same comparison as in Figure 6 except that postprocessing using Gaussian smoothing has been applied with a 400 km radius for the GRACE solutions. The blue curve represents the coefficients of the standard solution, the red curve represents the delta Stokes coefficients of the global 4° mascons, and the green curve represents the coefficients of the GLDAS surface hydrology model (no smoothing). Given that atmospheric pressure and tidal mass flux signals are forward modeled in these solutions, the expected spectra of the gravity fields would be similar to the spectrum of the global hydrology. These smoothed solutions have excess power in the middle degrees with the power rapidly falling off at the highest degrees.

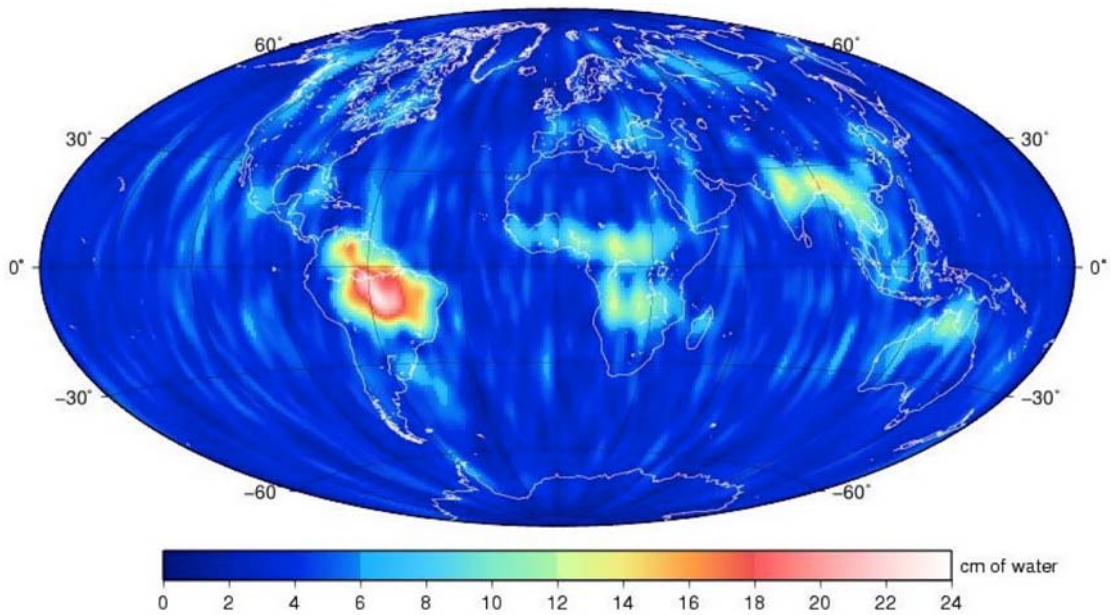

Figure 8. The standard deviation of surface mass (expressed in standing water height) obtained from 13 monthly solutions for the standard 60 × 60 unconstrained direct solution for Stokes coefficients. Atmospheric pressure and tidal mass flux have been forward modeled. The solution has been postprocessed using Gaussian smoothing with a radius of 400 km.

[2005] and *Luthcke et al.* [2008] are estimated every 10 days and employ temporal constraint equations in addition to spatial constraint equations. However, we are examining monthly solutions, and these do not require temporal constraint.

[21] Our mascon constraint equations are quite simple and very easy to implement. In a solution with N mascon parameters, there are $(N^2 - N)/2$ distinct pairs of mascon parameters and one constraint equation is written for each of these distinct pairs. For the pairing of mascon parameters

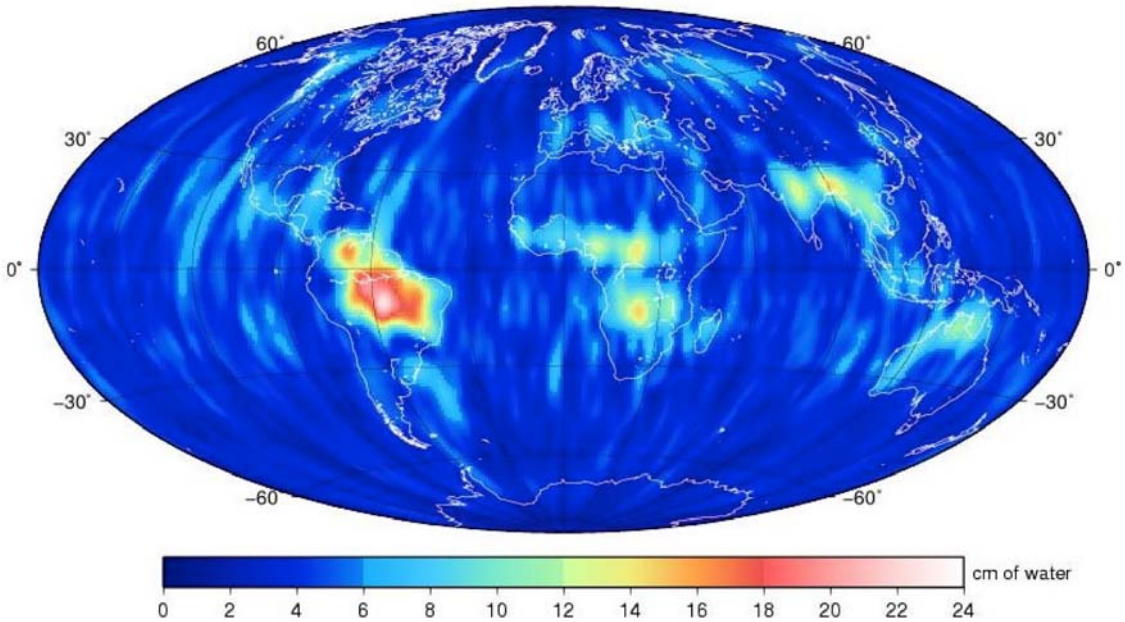

Figure 9. The standard deviation of surface mass (expressed in standing water height) obtained from 13 monthly solutions for the unconstrained 4° global mascon solution. Atmospheric pressure and tidal mass flux have been forward modeled. The solution has been postprocessed using Gaussian smoothing with a radius of 400 km.

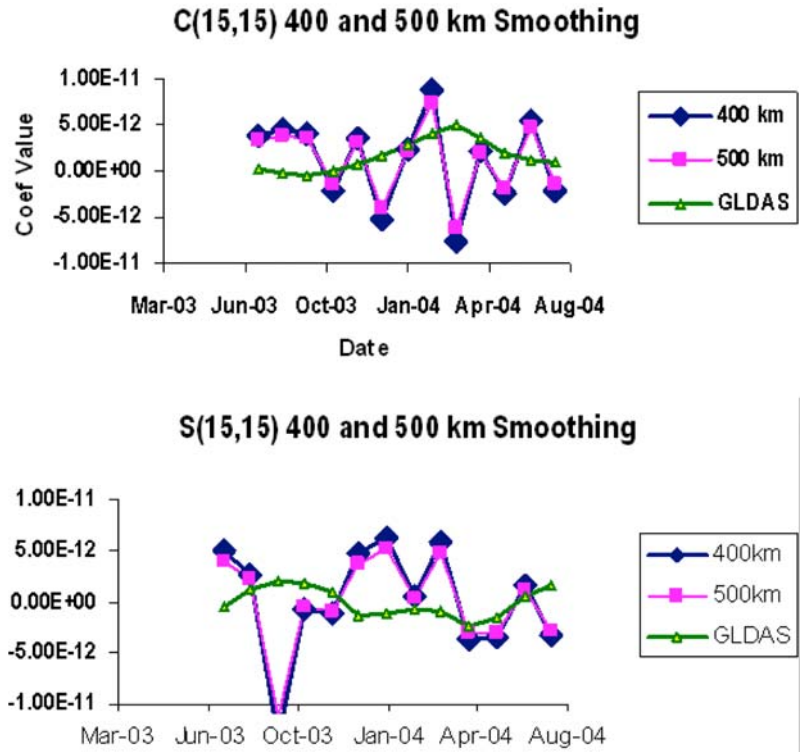

Figure 10. The resonance terms [$C(15, 15)$ and $S(15, 15)$] from the GRACE standard unconstrained spherical harmonic solution and from the GLDAS hydrology model. The coefficients from the GRACE solution have been Gaussian smoothed with a radius of 500 km and also with a radius of 400 km.

with numbers I and J (I is not equal to J and both I and J are greater than zero and less than N), the constraint equation takes the form:

$$P_I - P_J = 0. \tag{5}$$

To consider how equation (5) is added to (or summed into) our least squares normal equations, it is instructive to consider how each GRACE KBRR observation equation is summed into the normal equations. To sum a GRACE KBRR observation equation, four categories of items are required: an observation value, a theoretical (or computed) observation value (a residual is formed from the difference of the actual observation and the theoretical), partial derivatives of the theoretical observation with respect to all estimated parameters, and a weight for the equation. The tracking data analysis software computes theoretical observations and the associated partial derivatives. Each GRACE KBRR observation has a theoretical precision of 10^{-6} m/s, so we use a weight of 10^{12} (the reciprocal of the theoretical precision of the observation squared) for each KBRR observation equation.

[22] We treat our constraint equations almost exactly as the KBRR observation equations with the following three modifications: (1) the observed value is always zero, (2) the theoretical value is the left hand side of equation (5), and (3) the weight varies among the constraint equations and is determined by the relationship in time and space of the parameter pair for which the constraint equation is being written. The partial derivatives of each constraint equation are trivial to compute. The partials of all parameters except P_I and P_J are zero, and the partials of parameters P_I and P_J are one and negative one, respectively.

[23] The constraint equations are intended to produce a solution in which the difference between estimated values of pairs of neighboring (neighbors in space) mascon parameters is small. For spatial constraints, this is accomplished by the weighting of the constraint equations as given by equation (6).

$$WT_{IJ} = S \times \exp\left(1 - d_{ij}/D\right), \tag{6}$$

where WT_{IJ} is the weight given to the constraint equation for mascon parameters P_I and P_J; d_{ij} is the distance in kilometers between the centers of the regions corresponding to mascon parameters P_I and P_J; D is the correlation distance; and S is a scale factor chosen for the constraint equations.

[24] In practice, we create one set of least squares normal equations from the GRACE KBRR data and another set of normal equations from the constraint equations and then form a single set of normal equations by adding the two sets together. The scale factor, S, in equation (6) is chosen so that the diagonals of the normal matrix of the constraint equations are never more than 10% of the diagonals of the normal matrix of the KBRR observation equations. Typically, S is less than 0.001. The correlation distance, D, is usually chosen to be the length of a block (400 km for the solution currently being described). It should be noted that in this section we are describing a mascon time series

consisting of 13 individual monthly solutions. Therefore in this discussion, N (the number of mascon parameters) is 2856 with 13 separate solutions being made and not 13 × 2856 (as in one big solution over all 13 months).

[25] Figures 11a, 11b and 11c demonstrate that the spatial constraints with a correlation distance of 400 km have no influence on the long-wavelength aspect of the solution. Figure 12 shows that the constrained global mascon solution appears much more reasonable at degree and order 15 than the unconstrained versions shown in Figures 3d and 3e and the smoothed versions shown in Figure 10. The time series of these resonance terms from the embedded constraint are coherent and agree generally with GLDAS hydrology. Figures 13 and 14 show that in the global mascon solution with embedded constraints, a reasonable power spectrum is compatible with a reasonable distribution of mass signal.

[26] The constrained global mascon solution is a substantial improvement over either unconstrained solution, even after Gaussian smoothing has been applied. Apparently, the improvement is not gained because of the type of parameter being estimated, but by the fact that the smoothing is accomplished with constraint equations in the parameter estimation. With a single type of constraint equation applied between every distinct pair of mascon parameters within a monthly solution, we obtain reasonable smoothing, a reasonable power spectrum, and a sensible time series of resonance coefficients. In the next section, we will show how this global mascon solution can be improved.

5. The 2° Equal Area Global Mascons

[27] Although the constrained global mascon solution presented in the above section is an improvement over unconstrained solutions for both mascons and Stokes coefficients, it does not take full advantage of constraint equations. Monthly gravity solutions are degraded by gravity signal with variations that cannot be captured by parameters that are static over 30 days. Although the forward models used in these solutions mitigate this problem somewhat, it is helpful to estimate time variable gravity more frequently than once a month. Mascons are easy to use with time constraint equations that facilitate 10 day solutions (where each parameter is estimated from 10 days of KBRR data). The mascon solutions presented in the previous section were 30 day solutions to facilitate a comparison with standard monthly solutions for Stokes coefficients. The global mascon solutions presented in this section are estimated every 10 days and employ time constraint equations with a correlation time of 10 days.

[28] Each mascon parameter is assigned a time tag that is epoch at the center of the period (in this case, a 10 day period) with which it associated. The addition of the aspect of time to the constraint equations can be accomplished with two modifications to the procedure for implementation of spatial constraints discussed in the previous section. First, equation (6) is modified:

$$WT_{IJ} = S \times \exp\left(2 - d_{ij}/D - t_{ij}/T\right), \tag{7}$$

where WT_{IJ} is the weight given to the constraint equation for mascon parameters P_I and P_J; d_{ij} is the distance in kilometers between the centers of the regions corresponding to mascon parameters P_I and P_J; D is the correlation distance; t_{ij} is the difference in time tags (in days) of the mascon parameters P_I and P_J; T is the correlation time in days; and S is a scale factor chosen for the constraint equations.

[29] Similar to the correlation distance D, the correlation time, T is usually chosen to be the length of one block (in units of time, in this case 10 days). The second modification caused by the addition of the aspect of time is the grouping together of all mascon parameters from all time periods into one large inversion. As a practical matter this makes N, the number of mascon parameters in a single solution, much larger than when only spatial constraints are being applied and the number of constraint equations, $(N^2 - N)/2$, larger still (of course the number of solutions goes down to one). We are investigating a means to make such a large single inversion (405,444 mascon parameters), but our current algorithms and resources force us to make 13 individual solutions with three-time correlated periods within each of the solutions, but no time correlation between solutions.

[30] In this section, we hope to improve our mascon time series of by adding the aspect of time to the constraint equations. Although this requires one large inversion for the entire time series, a relationship between parameters at different time steps is established. We also hope to improve the estimated time series by withholding constraint equations that correspond to certain pairs of mascon parameters. The spatial constraints used in the previous section were suboptimal. Those constraint equations equate every block with every neighboring block. Over homogeneous areas, such as river basins or oceans, this is a useful constraint. Inevitably, though, land blocks are tied to adjacent ocean blocks and land blocks without glaciers are tied to blocks with glaciers. In other words, ties are made between regions that have different time variable gravity characteristics.

[31] The global mascon solution presented in this section divides the Earth into 25 regions including 6 ocean or inland sea areas and 19 land or land-ice areas. Table 1 lists the constraint regions.

[32] Within each region, the time variable gravity should be driven by similar hydrological, ocean, or ice phenomena. In the constrained global mascon solution of the previous section, there is a separate constraint equation corresponding to every distinct pair of blocks on the grid. In the solution described in this section, a constraint equation is written for a pair of distinct blocks, only if both blocks belong to the same region. This type of strategy is easier to implement when blocks are smaller because small blocks are more easily classified into regions. The mascons in this section are on a grid similar to the one of the previous section, except the spherical caps are 1° (not 2°) and the latitude bands are 2° (not 4°). This results in the estimation of 10,396 mascon parameters every 10 days.

[33] As before, each mascon block is represented by a set of spherical harmonic functions through degree 60. As explained in section 3, the vector space described by any set of mascons represented as spherical harmonics to degree 60 is completely described by 3720 linearly independent functions. Therefore, without the addition of spatial constraint equations any normal matrix formed for the 10,396 2° global mascons is rank deficient by a large margin.

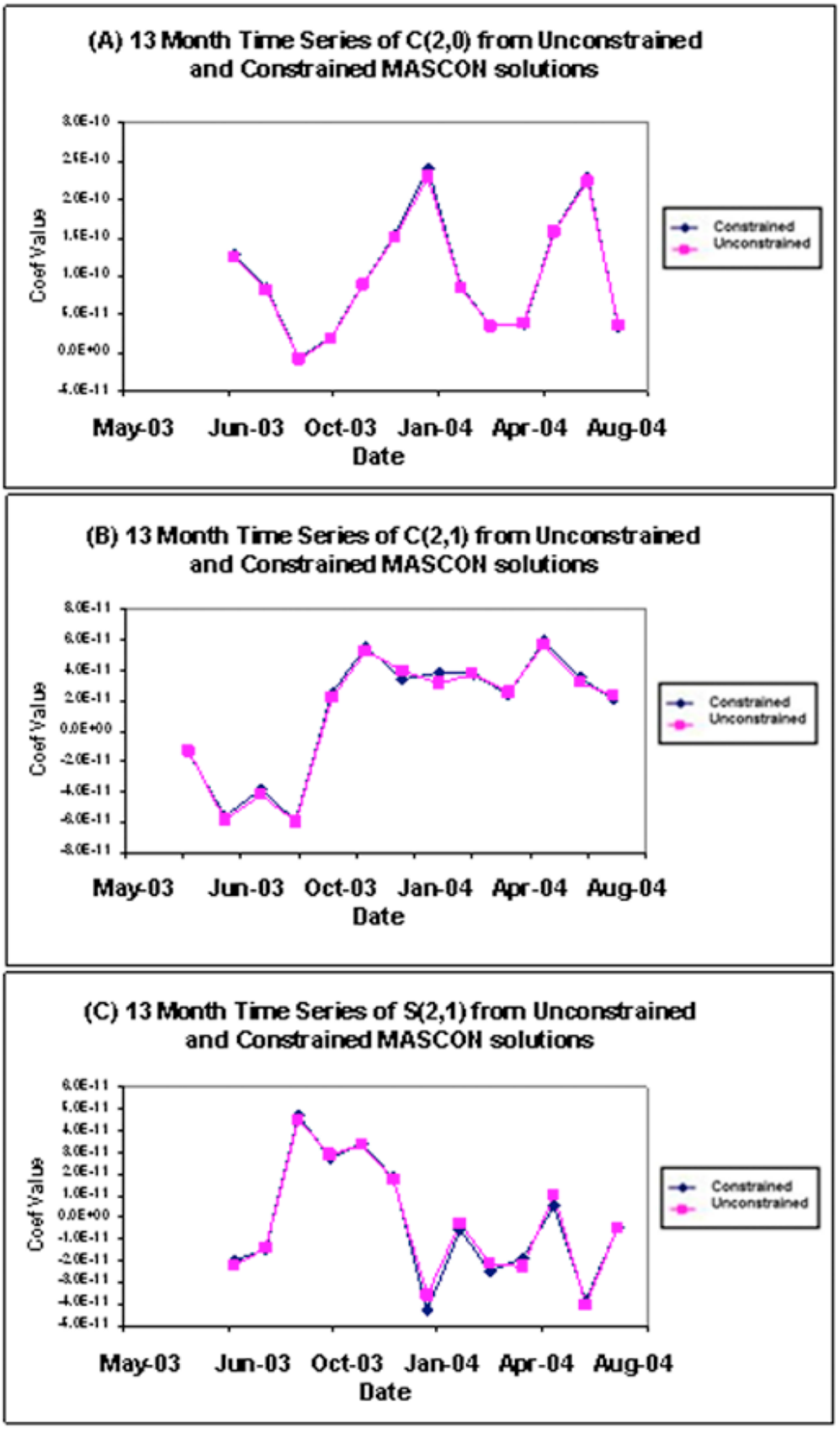

Figure 11. Spherical harmonic coefficients at degree 2 from two 4° global mascon solutions. One solution is unconstrained, and the other uses an embedded constraint (spatial constraint only). The constraint has almost no discernable effect on the long wavelength gravity model reconstituted from mascons.

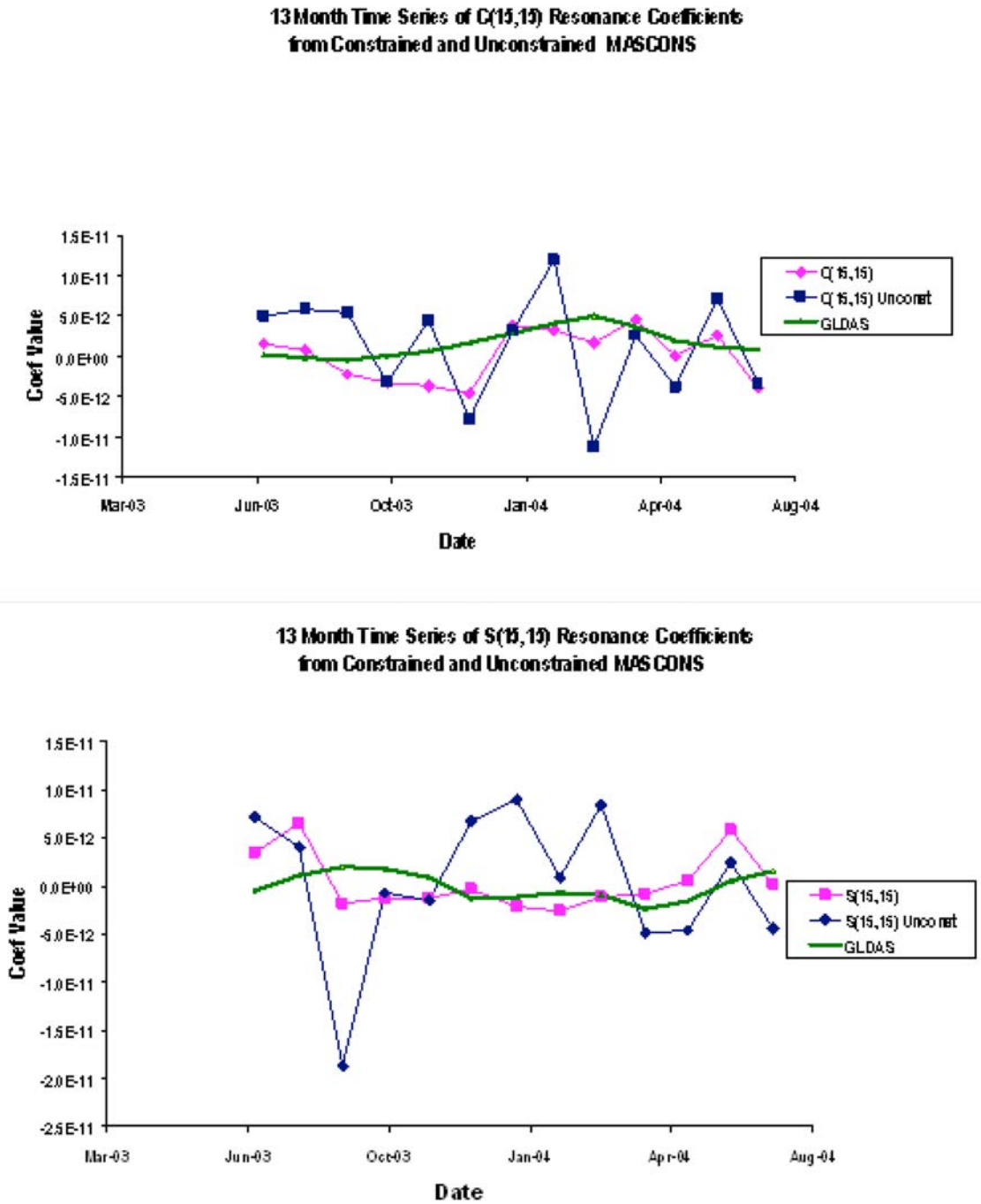

Figure 12. Spherical harmonic coefficients at the primary resonance of GRACE (degree 15 and order 15) from two 4° global mascon solutions and also from GLDAS hydrology. One of the GRACE solutions is unconstrained, and the other uses an embedded constraint (spatial constraint only). The constraint yields far more reasonable time variation for the resonance term revealing a near annual variation and much better agreement with GLDAS hydrology than both the unconstrained solution and the Gaussian smoothed solutions shown in Figure 10.

[34] Figure 15 shows that the 2° mascon solution captures a mass flux signal at a much higher resolution than either of the solutions in the previous section. For example, areas that are known to have significant mass flux signal such as coastal southwest and southeast Greenland, the Red Sea and the Caspian Sea are clearly isolated in Figure 15, but not in Figures 4, 5, 8, 9, and 13. In addition, Figure 16 shows that the power spectrum of the 2° solution is very reasonable when compared to that of global hydrology.

[35] Plotting the mass distribution from a mascon solution (as in Figure 15) brings up an interesting point that is related to Figure 1 and to the use of averaging kernels. Figure 1 demonstrates that a GRACE intersatellite KBRR observation cannot differentiate between two representations (one at

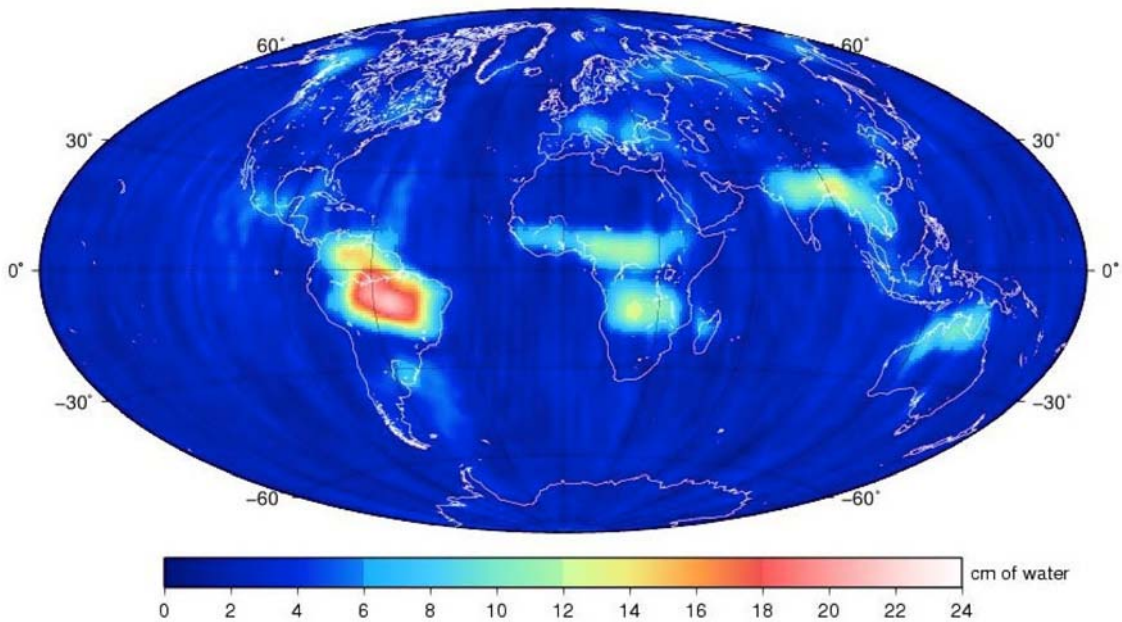

Figure 13. The standard deviation of surface mass (expressed in standing water height) obtained from 13 monthly 4° global mascon solutions estimated directly from the GRACE KBRR and using embedded spatial constraints in the estimation process.

degree 60 and the other at degree 120) of a reasonably sized mascon. The total surface mass is the same in these two representations, but at degree 60 the mass is spread out over an area larger than the original definition of the block. Although Figure 1 demonstrates the GRACE KBRR data are relatively insensitive to the exact boundaries of the

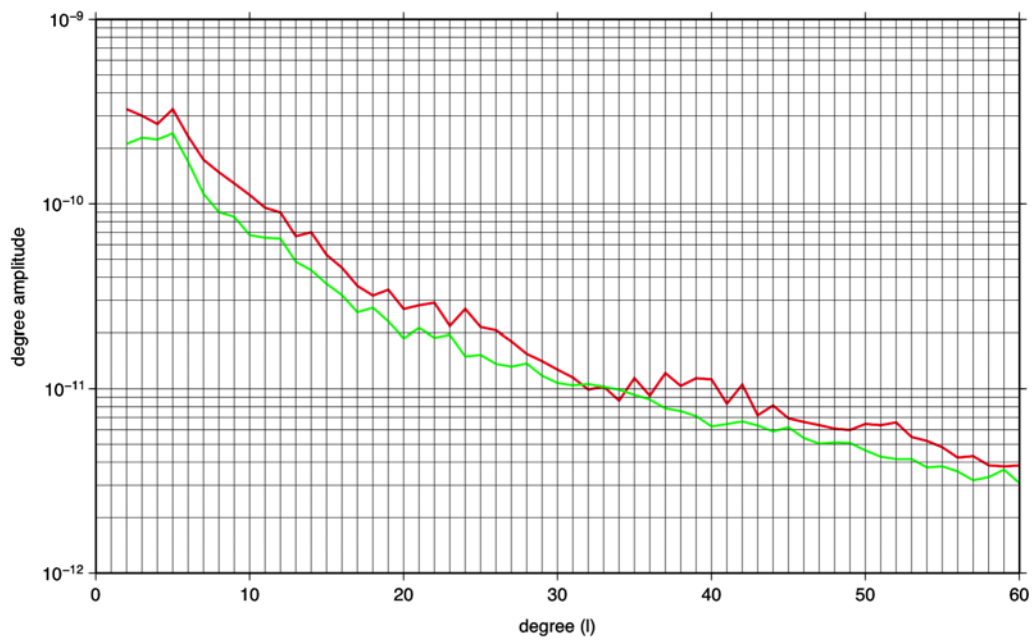

Figure 14. Power spectrum of changes with respect to the GGM02C gravity field and forward models from the constrained 4° global mascon solution compared to the GLDAS surface hydrology model. The red curve represents the delta Stokes coefficients of the global mascons, and the green curve represents the coefficients of the GLDAS surface hydrology model. Given that atmospheric pressure and tidal mass flux signals are forward modeled in these solutions, the expected spectrum of the mascon solution would be that arising from global hydrology. The constrained mascon solution has overall good agreement with the hydrological signal.

Table 1. Constraint Regions

	Regions
Ocean and Inland Sea	Mediterranean Sea, Black Sea, Hudson Bay, Caspian Sea, Global Ocean, and Red Sea
Land	North America, South America, West Eurasia, Africa, Australia, Madagascar, Japan, New Zealand, Philippines, Borneo, New Guinea, East Eurasia (including Sumatra), India, coastal Greenland, inland Greenland, costal Antarctica, inland Antarctica, Alaska glaciers, and various large Arctic islands north of Canada

mascon block, it does demonstrate that KBRR data detect the location of the center of the block quite well (the plot has perfect symmetry about the center of the mascon). During the reduction of KBRR data, we represent our mascons to (only) degree 60 because it is computationally convenient, but we attribute the mass implied by estimated mascon scale factor to the confines of its associated block (as if the mascon had been represented to degree 120). When we made the plot for Figure 15, we simply evaluated equation (4) at a dense set of points with the Stokes coefficients from the 2° global mascons reconstituted to degree 120. If the mass distribution is plotted using an expansion reconstituted to (only) degree 60, the estimated mass signal between adjacent mascon cells mixes. A representation of the mascons to degree 120 retains the original definition of each block much better than a representation to degree 60. Figures 17 and 18 show the mass flux signal of the 2° mascon solution over Greenland represented to degree 120 (Figure 17) and also to degree 60 (Figure 18). In the degree 120 representation, the signal stays mainly along the coastline with signal extending much less distance into the ocean and into the interior than the in the degree 60 representation. In the degree 120 representation, the largest signal is clearly concentrated on the locations of specific mascon cells on the southwestern and southeastern coasts. These are areas that are known to have significant mass flux [*Luthcke et al.*, 2006a]. In the degree 60 representation, the signal from these areas extends much further into the ocean.

[36] The situation described just above is very similar to the reason that averaging kernels with (postsolution) estimated scale factors are often used when computing mass flux from standard monthly Stokes coefficients. Monthly Stokes coefficients are often computed to at most degree 60. At this resolution, a significant portion of the computed mass flux from an area such as Greenland spills out onto adjacent areas, especially after Gaussian smoothing has been applied. A simulation is often performed to estimate the amount of mass flux that the computations have lost. The simulation gives an estimate of a scale factor that can be applied to the mass flux computations to compensate for the loss [*Swenson and Wahr*, 2002]. This averaging kernel scale factor is very much similar to a mascon parameter (which is also a scale factor); however, the mascon scale factor is estimated directly from the GRACE KBRR tracking data. As a parameter estimated directly from the fundamental observation, it introduces less uncertainty than a scale factor computed from simulations. The estimation of global mascons gives a means for producing Stokes coefficients that do not require Gaussian smoothing and do not need averaging kernels with scale factors in order to be used in mass flux computations.

6. Summary

[37] We have demonstrated that in unconstrained global gravity solutions derived from GRACE KBRR data, there is almost no difference between global mascon-based and

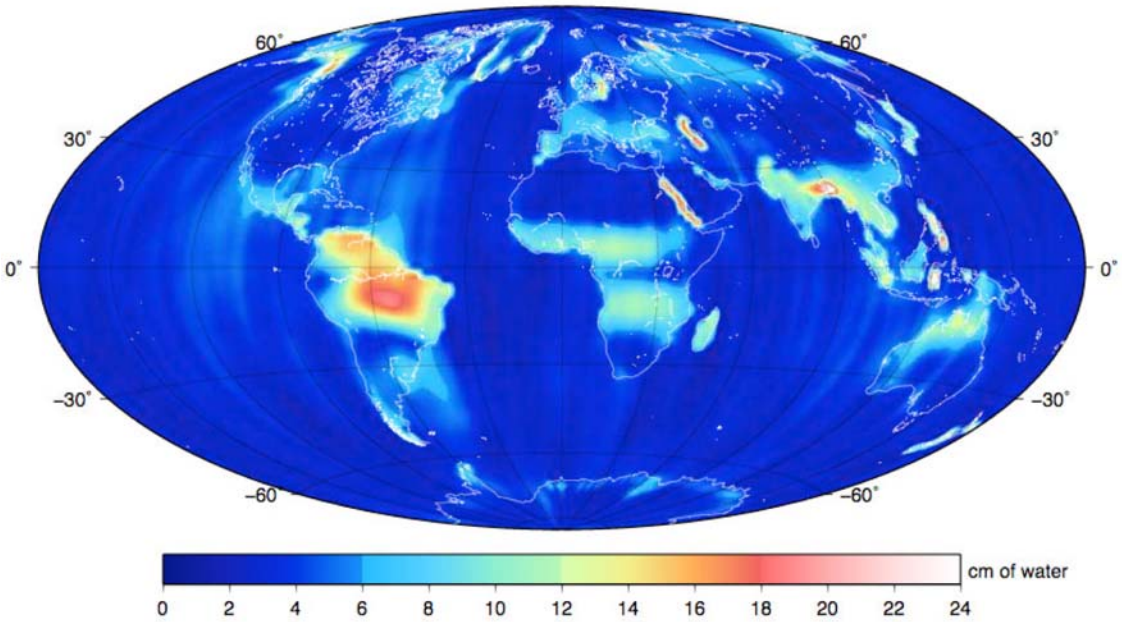

Figure 15. The standard deviation of surface mass (expressed in standing water height) obtained from 39 10 day 2° global mascon solutions from GRACE KBRR data. The solution uses both spatial and temporal constraints to estimate 10,396 2° mascons every 10 days.

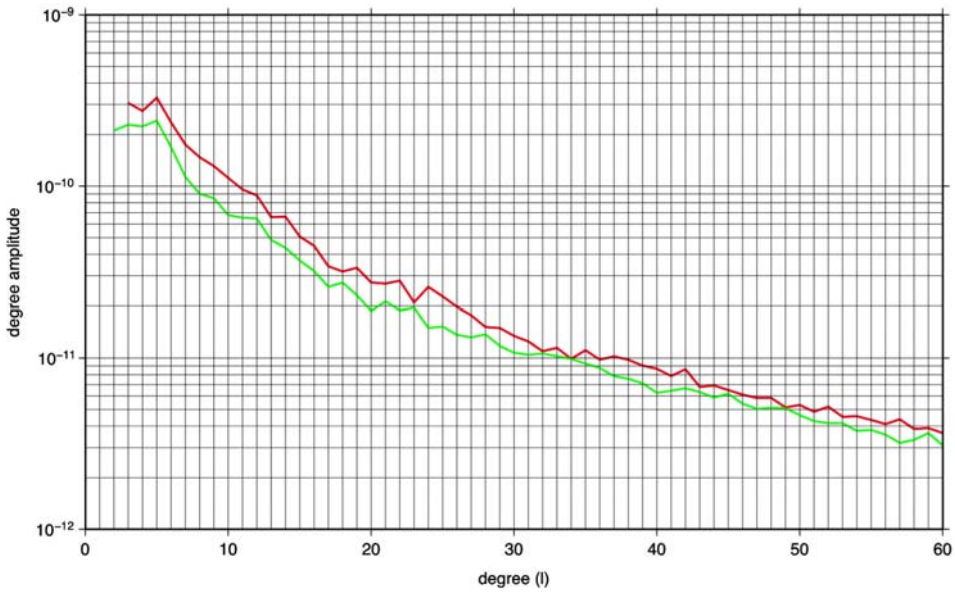

Figure 16. Power spectrum of changes with respect to the GGM02C gravity field and forward models of the constrained global 2° mascon solution compared to the GLDAS surface hydrology model. The red curve represents the delta Stokes coefficients of the global 2° mascons, and the green curve represents the coefficients of the GLDAS surface hydrology model. Given that atmospheric pressure and tidal mass flux signals are forward modeled in these solutions, the expected spectrum of the mascon solution would be that arising from global hydrology. The constrained 2° mascon solution has good overall agreement with the hydrological signal.

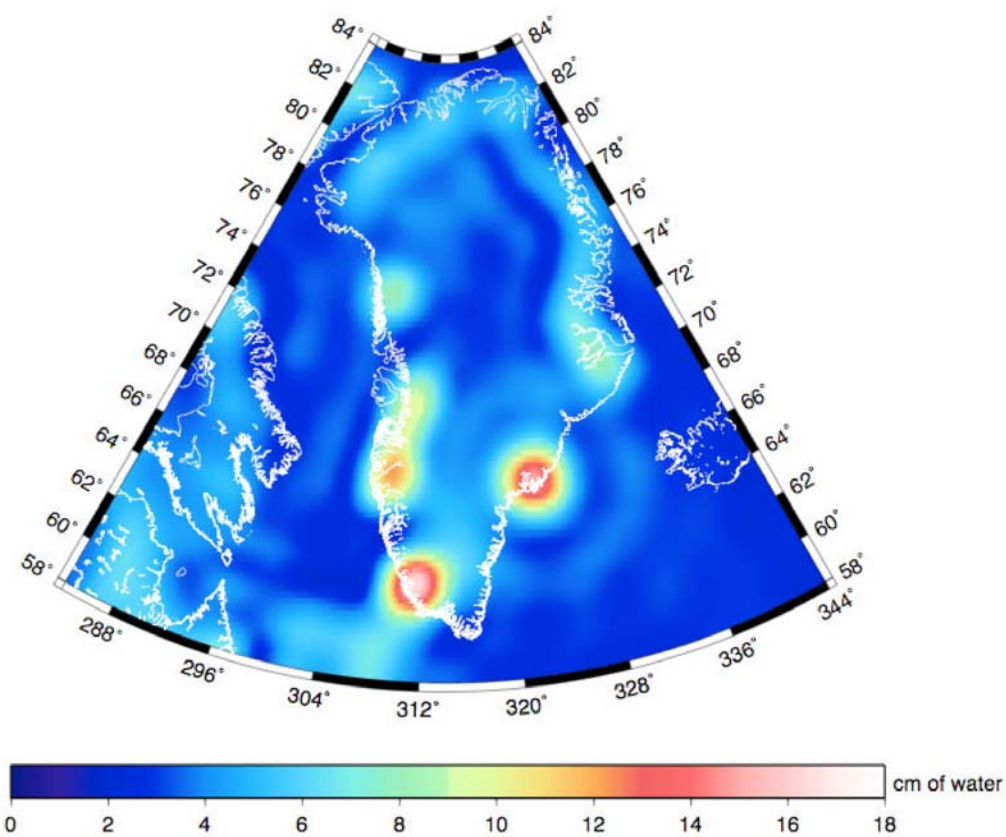

Figure 17. The standard deviation of surface mass (expressed in standing water height) over Greenland from the 2° mascon solution. Figure 17 differs from Figure 15 in that it is enlarged over Greenland and has been rescaled to show more detail (both Figures 15 and 17 are computed to degree 120).

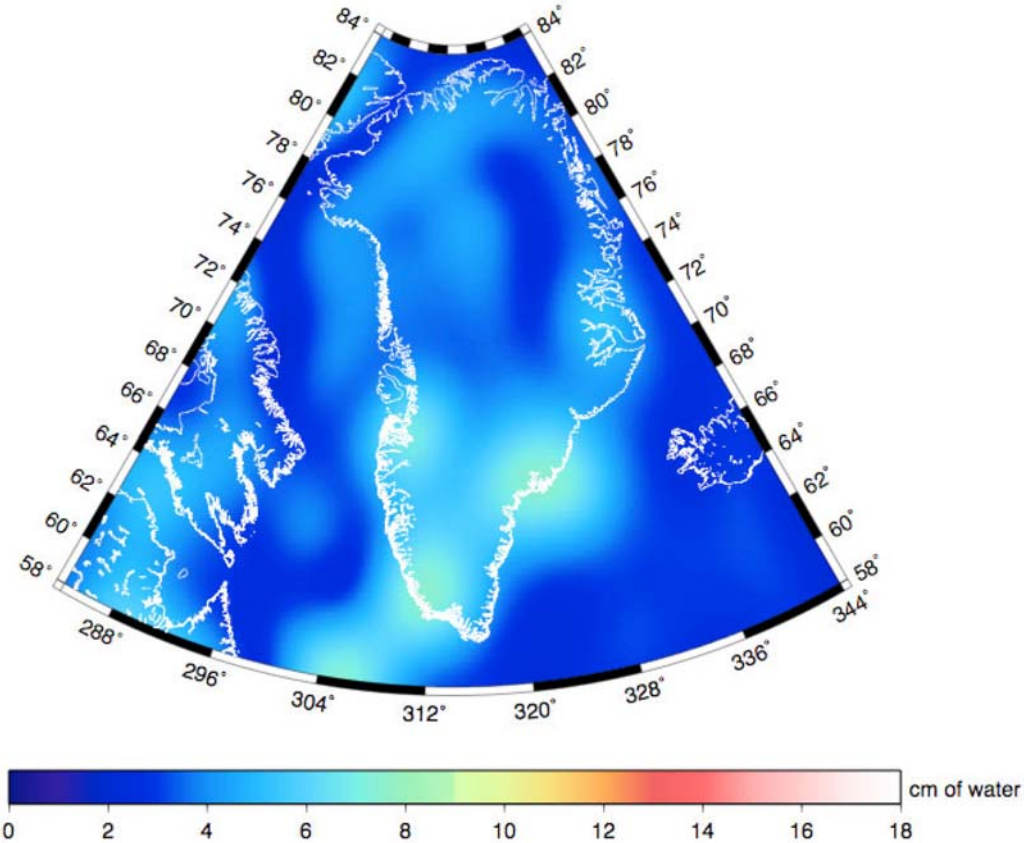

Figure 18. The standard deviation of surface mass (expressed in standing water height) over Greenland from the 2° mascon solution. Figure 18 differs from Figure 17 in that it is computed to only degree 60 (Figures 15 and 17 are computed to degree 120).

Stokes coefficient based approaches. We have also demonstrated that for mascons, smoothing using constraint equations embedded in the tracking data solution has advantages over Gaussian smoothing done after the tracking data solution. Smoothing done on mascons at the tracking data solution stage results in less signal loss. Presumably, the same would hold true in standard solutions for Stokes coefficients if the appropriate type of constraint equations would be applied. However, different equations at each degree and order would most likely be required. The high resolution of the mass flux derivations from mascons of *Luthcke et al.* [2006a] for Greenland and *Luthcke et al.* [2008] for Alaska as compared to other derivations in these areas that were based on Stokes coefficients can most likely be attributed to differences in smoothing techniques.

[38] We have also demonstrated that the estimation of Stokes coefficients through mascons (or as scale factors on sets of lumped Stokes coefficients) gives a way to produce gravity fields that are suitable for mass flux computations without the use of averaging kernels and postsolution scale factors. Finally, we have presented a preliminary solution for 2° equal area global mascons that is estimated every 10 days. We intend to continue work on this solution by identifying more regions in which homogenous forcing occurs while extending the globally constrained time series. We will also pursue the use of more complete forward modeling.

[39] **Acknowledgments.** Support for this work was provided by NASA through the GRACE Science team. We gratefully acknowledge the quality of GRACE Level 1B products produced by our colleagues at the Jet Propulsion Laboratory. We would like to thank Shin-Chan Han (UMBC and GSFC's Planetary Geodynamics Laboratory) for useful suggestions.

References

Carrere, L., and F. Lyard (2003), Modeling the barotropic response of the global ocean to atmospheric wind and pressure forcing—comparisons with observations, *Geophys. Res. Lett.*, *30*(6), 1275, doi:10.1029/2002GL016473.

Chao, B. F., W. P. O'Conner, A. T. C. Chang, D. K. Hall, and J. L. Foster (1987), Snow load effects on the Earth's rotation and gravitational field 1979–1985, *J. Geophys. Res.*, *92*(B9), 9415–9422, doi:10.1029/JB092iB09p09415.

Chen, J. L., M. Rodell, C. R. Wilson, and J. S. Famiglietti (2006), Low degree spherical harmonic influences on gravity recovery and climate experiment (GRACE) water storage estimates, *Geophys. Res. Lett.*, *32*, L14405, doi:10.1029/2005GL022964.

Luthcke, S. B., H. J. Zwally, W. Abdalati, D. D. Rowlands, R. D. Ray, R. S. Nerem, F. G. Lemoine, J. J. McCarthy, and D. S. Chinn (2006a), Recent Greenland ice mass loss by drainage system from satellite gravity observations, *Science*, *314*(1286), 1286–1289, doi:10.1126/science.1130776.

Luthcke, S. B., D. D. Rowlands, F. G. Lemoine, S. M. Klosko, D. Chinn, and J. J. McCarthy (2006b), Monthly spherical harmonic gravity field solutions determined from GRACE inter-satellite range-rate data alone, *Geophys. Res. Lett.*, *33*, L02402, doi:10.1029/2005GL024846.

Luthcke, S. B., A. A. Arendt, D. D. Rowlands, J. J. McCarthy, and C. F. Larsen (2008), Recent glacier mass changes in the Gulf of Alaska region from GRACE mascon solutions, *J. Glaciol.*, *54*(188), 767–777, doi:10.3189/002214308787779933.

Muller, P. M., and W. L. Sjogren (1968), MASCONS—lunar mass concentrations, *Science*, *161*(3842), 680–684, doi:10.1126/science.161.3842.680.

Rapp, R. H. (1974), Procedures and results related to the direct determination of gravity anomalies from satellite and terrestrial gravity data, *OSU Rep. 211*, Ohio State Univ., Columbus.

Ray, R. D. (1999), A global ocean tide model from TOPEX/POSEIDON altimetry: GOT99.2, *Tech. Rep. 1999–209478*, NASA, GSFC, Greenbelt, Maryland.

Ray, R. D., and R. M. Ponte (2003), Barometric tides from ECMWF operational analyses, *Ann. Geophys.*, *21*, 1897–1910.

Rodell, M., et al. (2004), The global land data assimilation system, *Bull. Am. Meteorol. Soc.*, *85*(3), 381–394, doi:10.1175/BAMS-85-3-381.

Rowlands, D. D., R. D. Ray, D. S. Chinn, and F. G. Lemoine (2002), Short-arc analysis of intersatellite tracking data in a gravity mapping mission, *J. Geod.*, *76*, 307–316, doi:10.1007/s00190-002-0255-8.

Rowlands, D. D., S. B. Luthcke, S. M. Klosko, F. G. Lemoine, D. S. Chinn, J. J. McCarthy, C. M. Cox, and O. B. Anderson (2005), Resolving mass flux at high spatial and temporal resolution using GRACE intersatellite measurements, *Geophys. Res. Lett.*, *32*, L04310, doi:10.1029/2004GL021908.

Rummel, R., D. Hajela, and R. Rapp (1978), Recovery of mean gravity anomalies from satellite-satellite range rate data using least squares collocation, *OSU Rep. 248*, Ohio State Univ., Columbus.

Swenson, S., and J. Wahr (2002), Methods for inferring regional surface-mass anomalies from gravity recovery and climate experiment (GRACE) measurements of time-variable gravity, *J. Geophys. Res.*, *107*(B9), 2193, doi:10.1029/2001JB000576.

Swenson, S. C., and J. Wahr (2006), Post-processing removal of correlated errors in GRACE data, *Geophys. Res. Lett.*, *33*, L08402, doi:10.1029/2005GL025285.

Tapley, B. D., S. V. Bettadpur, M. Watkins, and C. Reighber (2004), The gravity recovery and climate experiment mission overview and early results, *Geophys. Res. Lett.*, *31*, L09607, doi:10.1029/2004GL019920.

Tapley, B., et al. (2005), GGM02—An improved Earth gravity field model from GRACE, *J. Geod.*, *79*(8), 467–478, doi:10.1007/s00190-005-0480-z.

Velicogna, I., and J. Wahr (2006), Acceleration of Greenland ice mass loss in Spring 2004, *Nature*, *433*, 329–331, doi:10.1038/nature05168.

Wahr, J., M. Molenaar, and F. Bryan (1998), Time variability of the Earth's gravity field: Hydrological and oceanic effects and their possible detection using GRACE, *J. Geophys. Res.*, *103*(B12), 30,205–30,229, doi:10.1029/98JB02844.

Wong, L., G. Buechler, W. Downs, W. Sjogren, P. Muller, and P. Gottlieb (1971), A surface-layer representation of the lunar gravitational field, *J. Geophys. Res.*, *76*(26), 6220–6236, doi:10.1029/JB076i026p06220.

Wouters, B., D. Chambers, and E. J. O. Schrama (2008), GRACE observes small-scale mass loss in Greenland, *Geophys. Res. Lett.*, *35*, L20501, doi:10.1029/2008GL034816.

J.-P. Boy, EOST-IPGS, UMR 7516, Université de Strasbourg, CNRS, 5 Rue Descartes, F-67084 Strasbourg, France.

D. S. Chinn, S. M. Klosko, and J. J. McCarthy, SGT Inc., 7701 Greenbelt Rd., Ste. 400, Greenbelt, MD 20770, USA.

F. G. Lemoine, S. B. Luthcke, D. D. Rowlands, and T. J. Sabaka, Planetary Geodynamics Laboratory, Code 698, NASA Goddard Space Flight Center, Greenbelt, MD 20771, USA. (david.d.rowlands@nasa.gov)